

## ECT Studies of Bead Fluidization in Vertical Mills

David M. Scott and Oliver W. Gutsche

DuPont Central Research & Development, Experimental Station  
PO Box 80304, Wilmington, Delaware 19880-0304 USA  
scottdm@esvax.dnet.dupont.com

**ABSTRACT** – Vertical media mills require sufficient fluidization of the grinding media in order to be efficient. Fluidization is determined by the agitator speed and, in the case of recirculating mills, also by the flow rate through the recirculation pump. Inadequate fluidization lowers the efficiency of the mill, and excessive flow through the mill causes hydraulic packing at the output screen. The optimum operating conditions (agitator speed and flow rate) for such mills are presumed to be those which evenly distribute the grinding media throughout the mill. Electronic Capacitance Tomography (ECT) has been used to determine the media packing (beads per unit volume) and bead fluidization in an agitated vertical mill. The tomographic data is used to measure average packing along the axis and radius of a vertical mill for a number of agitation speeds. Several geometries and bead/fluid combinations have been studied. The results of this study are being used to identify optimal operating conditions instead of performing an extensive series of grinding experiments.

**Keywords:** ECT, fluidization, milling, process optimization

### 1. INTRODUCTION

Agitated media mills are used throughout industry for size reduction and dispersion of pigments, polymers, pharmaceuticals, and agricultural chemicals [1]. Such mills use pin or disk agitators to fluidize a bed of grinding beads, which typically fill 80% of the volume of the grinding chamber. The nominal size of these grinding beads (i.e., the media) ranges from 0.5 - 3 mm, and the beads may be glass, ceramic, or metallic. The slurry to be milled fills the remaining volume in the chamber. Energy is transmitted from the agitator to the liquid phase, which accelerates the beads; particles in the slurry break when they are nipped between colliding beads [2].

Media mills may be batch or continuous types. Batch mills are essentially stirred vessels where the total charge of slurry remains in the grinding chamber. In continuous mills, the slurry is pumped into the head plate, through the mill, and out through a media retainer screen. Continuous mills can be operated with the agitator mounted horizontally or vertically, and the slurry is often recirculated through the mill for maximum effect.

Optimum grinding or energy utilization occurs in an agitated bead mill when the grinding media is uniformly distributed throughout the mill [3]. From experience we know that when the flow rate of the slurry through the mill exceeds a critical value, grinding beads begin to pack at the retainer screen, causing screen wear, media wear, an increase in power consumption, and an overall decrease in grinding efficiency. Likewise,

if the beads are not fully fluidized, they remain on the bottom of the mill and wear grooves into the chamber walls; grinding under such conditions is ineffective. Successful grinding requires both effective particle capture and sufficient impact intensity. Bead fluidization influences both capture statistics and collision intensity, and therefore it is a prerequisite for optimum grinding.

Process parameters such as bead size, bead density, bead filling, fluid viscosity and rotational speed define the state of fluidization. The objective of this work is to monitor the bead distribution in batch and continuous agitated media mills in order to quantify the bead fluidization. Here we report on the application of electrical capacitance tomography (ECT) [4] to measure axial and radial bead distributions as well as overall bead fluidization in vertical media mills. This technique provides a tool to determine the optimum process conditions for grinding in agitated mills.

The ECT technique has been used by previous authors to study fluidization in the case of solids suspended by flowing gas. Rhodes et al. [5] recently investigated the flow structure formed by solids in a circulating fluidized bed. Dykowski [6] and Kühn et al. [7] measured the voidage in fluidized beds with ECT and used the voidage distribution to calculate the Kolmogorov entropy as a function of position and operating conditions. This data was used to characterize the structure of the bed.

We are not aware of any previous ECT studies that investigated bead fluidization in agitated solid/liquid systems such as vertical

mills. A closely related technique, Electrical Resistance Tomography, has been used to develop models of solid/liquid mixing in stirred tanks [8].

## 2. EXPERIMENTAL APPARATUS

### 2.1 Vertical mill

The vertical mill used in this study is depicted in Figure 1. It consists of a Plexiglass tube with outer diameter (OD) 14.6 cm and inner diameter (ID) 13.3 cm. The total length of the tube is 50.8 cm. A Plexiglass plate is cemented inside the tube at a distance of 11.4 cm from the bottom; this plate defines the bottom of the milling volume. This design provides physical access for placing the sensing plane of the ECT sensor (described below) at the bottom of the grinding chamber.

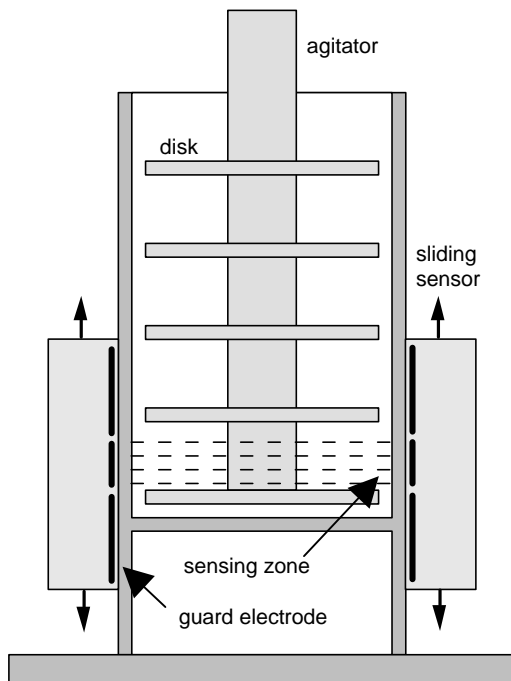


Figure 1: Cross section of the vertical mill.

The mill is open at the top, and the agitator is inserted into the mill through this opening. The purpose of the agitator is to fluidize the grinding beads and to supply them with the kinetic energy needed to break the particles in the slurry. The shaft of the agitator is connected to a variable speed motor (not shown) via a torque transducer. This transducer measures torque and rotational speed so that the power input to the mill can be determined.

Three different agitators were used in this study. They are similar to typical designs actually used in industrial mills. To be compatible with the ECT sensor, they were constructed of Delrin® engineering polymer.

The “disk” agitator (shown in Figure 1) has five removable solid disks, each 12.8 cm in diameter and 0.6 cm thick. The disks are centered on a 2.5 cm diameter shaft, with a gap of 10 cm between the disks. The agitator is mounted so that the bottom disk (on the end of the shaft) is suspended 0.5 cm above the bottom of the grinding chamber.

The “modified disk” agitator is very similar to the disk agitator. The diameter of the disks is smaller (10 cm), but the disk thickness and spacing are not changed. Each of the modified disks has three large holes (covering about 15% of the surface) in it. The intended purpose of these holes is to improve the axial flow in the mill.

The “pin” agitator has a shaft 2.5 cm in diameter, with six 1.3 cm diameter pins (i.e., rods) installed in mounting holes drilled through the shaft at right angles. The pins are 10 cm long, and they are mounted in an alternating pattern (E-W, N-S, E-W, etc.) along the shaft; the spacing between pins is 7.5 cm.

### 2.2 Tomographic sensor

The sensor used in this study is a electrical capacitance tomography (ECT) system built by Process Tomography Ltd. (Wilmslow, Cheshire, U.K.). This unit was purchased several years ago for pneumatic conveying studies [9], but it has also been used for investigations of fluidized beds. The sensor array used here was designed to image bubbles in a bed of polymer powder fluidized with air.

The sensor has an ID of 15.2 cm and stands about 23 cm tall. It fits around the vertical mill housing and can slide along the axis of the mill. The sensor is supported by wooden blocks, so that its axial position can be changed with ease.

This sensor has eight 3 cm X 5.5 cm sensor electrodes and sixteen 10 cm X 5.5 cm driven guard electrodes [4]. The sensor electrodes define the sensing plane and are mounted in the middle of the sensor, as shown in Figure 1. The purpose of the driven guards is to improve the axial spatial resolution of the sensor by preventing the formation of a fringing field near the sensors. Three dimensional calculations of the electric field and resulting capacitance show that, while the guard electrodes lower the sensitivity to the out-of-plane dielectric distribution, they do not completely prevent out-of-plane disturbances from interfering with the tomographic images. This aspect of ECT imaging has an impact on measurements of the axial distribution of grinding beads, as discussed below.

The ECT system was used to measure several parameters (radial distribution of beads, axial distribution of beads, and fluidization at specific heights in the vertical mill) as a function of agitator type and speed. The system

generates cross sectional images based on a calibration of permittivity. The calibration was performed with the continuous phase (oil) as the low permittivity material (0% packing) and a packed bed of grinding beads in the continuous phase as the high permittivity material (100% packing). The gray levels in the reconstructed images measure the bead density (bead packing fraction) as a function of position.

The radial bead distribution is determined by casting the ECT cross-sectional image into polar coordinates and integrating around the polar angle. Wall effects near the electrodes complicate the interpretation of the radial distribution data.

In order to determine the axial distribution of grinding beads, the cross-sectional image is integrated to determine the average bead packing fraction at that axial position under those experimental conditions. The sensor is then repositioned at another height (above the bottom plate) and another measurement is taken. The spatial resolution along the axis is limited by the size of the electrodes [10]. Near the bottom of the bed, there is some distortion due to the out-of-plane effects of the air under the column. (The suggestion has been made to fill the space under the column with a packed bed of beads and oil in order to reduce this effect, but that experiment has not been tried.) Deconvolution algorithms can improve the results, but for this study we have opted for a simple normalization procedure based on axial data for a packed bed. Near the top of the oil, the vortex formed by the agitator also causes some distortion of the axial distribution, so measurements are taken below the vortex.

An effective and robust measurement is to monitor the fluidization at a particular axial position as a function of agitator speed. This measurement avoids difficulties caused by position-dependent sensitivity and convolution effects. Fluidization is related to the bead packing fraction, which under the these experimental conditions varies from a value of 1.0 for a fully packed bed to a value of 0.8 for complete fluidization. Lower values of bead packing are measured near the top of the mill, where fewer beads are seen. For the purpose of this study we have defined the fluidization  $f$  at a given height as a function of the bead packing fraction  $p$  (measured via ECT):

$$f = 5(1 - p) \quad (1)$$

### 2.3 Experimental conditions

Although some ECT systems [11] are able to image gas bubbles in water, the sensor used here was designed for materials (polymer and air) with dielectric constants ( $\epsilon$ ) in the range of 1 - 3. The original intent in this study was to use

aqueous slurries, but they proved to be incompatible with this ECT system. In order to circumvent this problem, it was decided to use corn oil ( $\epsilon_{DC}=3.3$  [12]) instead of water ( $\epsilon_{DC}=80.0$ ) as the continuous phase. The corn oil replaced the aqueous slurry of particles that would normally be present in the mill.

The ceramic grinding beads used in this study were nominally 1 mm in diameter. Since the mill was open at the top (an unconstrained surface), the grinding volume was defined by the volume of the charge (beads plus oil). For this study, 1.2 liters of oil and 1.6 liters of beads were used, which combine to give a volume of 2.0 liters. The beads occupied 80% of the total charge volume, which is a typical loading for media milling operations. About half of the volume occupied by packed beads is free space (located between the beads), so the volume concentration of packed beads in oil is 50%. When the beads are fully fluidized, the volume concentration of beads in the oil is about 40%.

## 3. EXPERIMENTAL RESULTS

### 3.1 Radial distribution of beads

Cross-sectional ECT images of the mill provided the information to determine the radial distribution of the grinding beads. A typical result is shown in Figure 2. The centripetal force imparted by the agitator tends to push the beads outwards (towards the wall of the mill), increasing the bead fraction. This effect is clearly seen in the Figure.

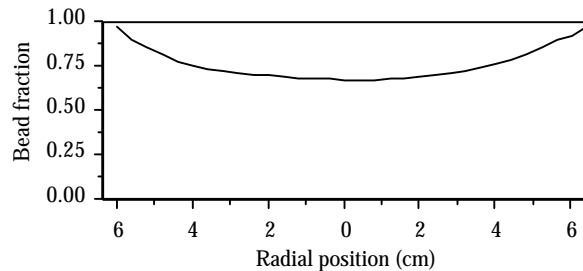


Figure 2: Radial distribution of beads.

The agitator is not evident in the cross-sectional images or in the radial distribution data. There are several reasons for this effect: The spatial resolution in the sensing plane is about the same size as the agitator shaft, and these sensors are known to have a low sensitivity at the center of the tube [13]. Since the ECT calibration is performed with the agitator in place, these factors make it difficult to image the agitator shaft. This effect has no significance for the axial distribution and fluidization measurements.

### 3.2 Axial distribution of beads

The axial distribution was determined by integrating the bead fraction across the sensing plane at a given axial position. Near the top and bottom of the mill some distortion was evident, as discussed above.

Figure 3 shows the axial distribution of beads for the pin agitator at a speed of 586 rpm. The first 3 data points in this data have been normalized to axial data for a packed bed. This data shows partial (70%) fluidization over the lower 8 cm. Due to gravitational effects, the top portion of the mill has a relatively low bead fraction. Averaging the bead fraction over the height of the mill gives a value of about 80%, the value expected from conservation of bead volume. This result suggests that the calibration and normalization procedures do not introduce any large errors into the bead fraction measurement.

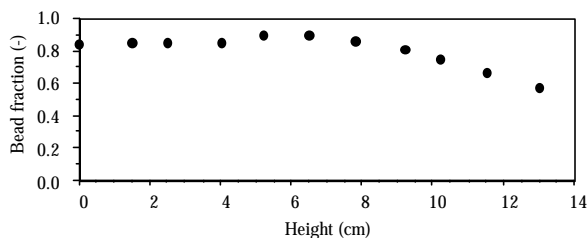


Figure 3: Bead packing as a function of axial position.

### 3.3 Measurement of fluidization

Representative data are shown in Figure 4 for fluidization in a mill using the pin agitator. A packing density of 1.0 denotes a fully packed state, whereas a value of 0.8 denotes complete fluidization (i.e., the beads are fully dispersed in the oil). The measurements at 2.5 cm and 5.1 cm from the mill bottom indicate that the lower portion of the bed does not begin to fluidize until the agitator speed exceeds 150 rpm. Full fluidization is reached at about 400 rpm, where the packing density reaches its plateau value of 0.8.

At very high agitator speeds, the air vortex is sucked down to the level of the sensor; the presence of the vortex (which can be seen in the tomographic image) alters the calibration of the sensor, leading to erroneously low readings. The position 10.2 cm from the bottom is quite close to the top of the packed bed, so it fluidizes at low agitator speed. At 300 rpm, the vortex has already formed in the upper region of the mill and has begun to interfere with the calibration of the sensor at that position. However, it is clear that the top of the bed begins to fluidize even at speeds as low as 50 rpm (a tip speed of 0.33 m/s).

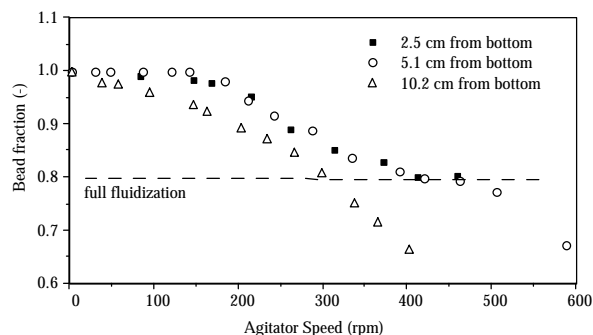


Figure 4: Packing density as a function of agitator speed for the pin agitator.

By recording the torque and speed of the agitator, one can determine the total power input. Figure 5 shows the fluidization (measured at a point 2.5 cm above the bottom) as a function of input power for the pin agitator. Here the fluidization is shown as a number ranging from 0-100% where 0% corresponds to the packed state (packing fraction 1.0), and 100% corresponds to the fully fluidized state (i.e., packing fraction 0.8 at this loading level). Thus we can directly quantify the fluidization of the particle system.

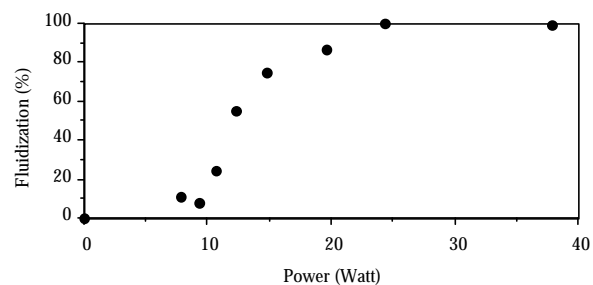


Figure 5: Fluidization as a function of input power for pin agitator.

### 3.4 Comparison of agitator efficiency

It is interesting to compare the efficiency of various agitator design using this technique. Figure 6 compares the packing density (measured at 5.1 cm) versus agitator speed for the pin and disk agitators. Neither design fluidizes the media well until speeds over 130 rpm (a tip speed of about 0.9 m/s) are reached. In both cases, the fluidization reaches a plateau between 300-500 rpm. The pin agitator completely fluidizes the media, but according to these results the disk agitator only partially fluidizes the media. It was noted during the experiment that the media were not well dispersed near the top of the column, which supports the recorded data. It appears that the beads were held up in the compartments between disks; in fact, after changing the speed it was necessary to wait for at least 30 seconds before the bead packing fraction stabilized. However, the fluidization is quite low (only 35%) which suggests that the instrument calibration for

that particular experimental run may have been inaccurate.

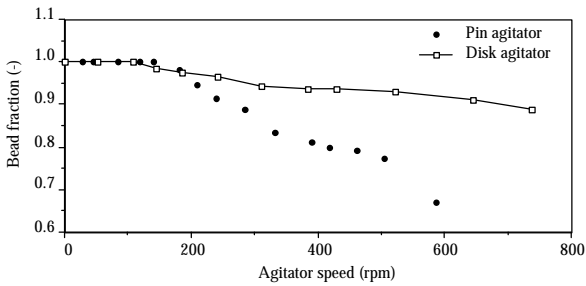


Figure 6: Packing density as a function of speed for pin and disk agitators.

Figure 7 depicts the packing fraction measured at 5.1 cm for the modified disk agitator. In contrast to the other two agitators, the modified disk begins to fluidize the bed even at very low agitator speeds. The bead packing fraction decreases linearly with speed in Figure 7, whereas in Figure 6 the packed bed does not start to fluidize until 150 rpm is reached. This result is attributed to improved axial flow due to the holes in the agitator disks. Thus, the modified disk agitator was observed to be the most effective design for fluidizing the media under these conditions.

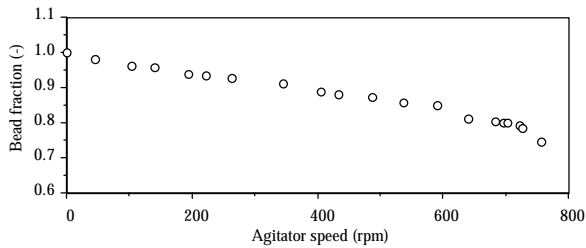


Figure 7: Packing density as a function of speed for modified disk agitator.

#### 4. DISCUSSION

In mixing practice, the fluid flow is characterized by a Reynolds number ( $Re$ ), and the agitator power is expressed in terms of the dimensionless Newton number ( $Ne$ ). The Reynolds number is defined in Equation (2) in terms of the agitator speed ( $n$ ), the agitator diameter ( $D$ ), the density of the fluid ( $\rho$ ), and the fluid viscosity ( $h$ ):

$$Re \equiv \frac{n \cdot D^2 \cdot \rho}{h} \quad (2)$$

The Newton number, defined in Equation (3), is the agitator power ( $P$ ) scaled by the density and the agitator diameter and speed. The Newton number is the drag force divided by the dynamic pressure or the drag coefficient. In the laminar

region the drag coefficient is inversely proportional to the Reynolds number.

$$Ne \equiv \frac{P}{\rho \cdot n^3 \cdot D^5} \quad (3)$$

Figure 8 shows the Newton number as a function of the Reynolds number for a pin agitator. Filled symbols represent data from a horizontal batch mill. The data exhibit a laminar region with a slope of one and a laminar-turbulent transition region with a slope less than one. Data for a vertical batch mill with a free surface is represented by the open triangles. In the laminar region  $Ne$  is strongly dependent on  $Re$ , and the slope of the curve exceeds unity. At  $Re=1100$  the triangles appear to merge with the laminar curve; at  $Re=1300$  a laminar-turbulent transition region is reached. To avoid formation of a vortex, the largest Reynolds number in our experiments was limited to 1700; therefore the behavior at larger  $Re$  values could not be investigated.

At low  $Re$  values, the deviation of  $Ne$ - $Re$  data from a slope of one is due to insufficient fluidization in the vertical batch mill. High  $Ne$  numbers result from higher power draw due to media-agitator friction. The magnitude of  $Ne$  is a measure of the degree of fluidization.

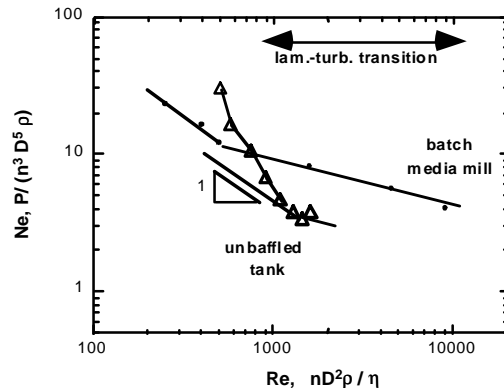


Figure 8: Newton number versus Reynolds number for the pin agitator. Filled symbols present data from a horizontal batch media mill [3].

Figure 9 shows bead fluidization as a function of the Newton number. The reverse S curve shows that high power is required at low fluidization. The excess power is required to accelerate the grinding beads. In practice, one could measure  $Ne$  (at a fixed Reynolds number) and determine the state of fluidization from a graph such as Figure 9.

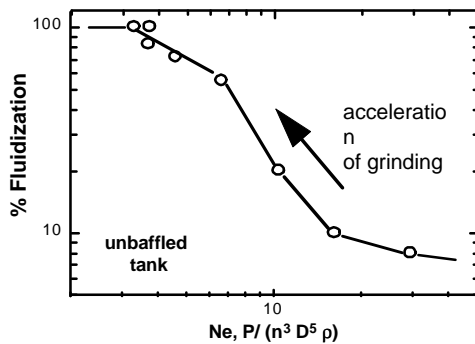


Figure 9: Fluidization versus Newton number (drag coefficient) for the pin agitator.

These results demonstrate several different types of analysis one can make on such mills using ECT sensors. In particular, we have been able to quantify the fluidization obtained under various operating conditions, and we have been able to compare the efficiency of different agitator designs. This technique is a valuable tool for optimizing media milling operations.

Future work will study the effects of fluid viscosity and media loading on fluidization. A continuous vertical mill is being built to study the phenomenon of hydraulic packing; it will also provide a closed system where the air vortex will not interfere with the tomographic measurements.

## ACKNOWLEDGEMENTS

The authors thank Mukesh Sharma, Ed Jochen, and John Harrington for their help in performing these experiments. A special thanks is due to Rick Nopper in our Modeling group for his calculations of the electrical field and capacitance in the driven guard sensor.

## REFERENCES

[1] Oliver Gutsche, "Size Reduction and Particle Dispersion in the Chemical Industry", International Comminution Research Association, Toulouse, France (1998).

[2] Arno Kwade, "Wet Comminution in Stirred Media Mills- Research and its Practical Application", 9th. European Comminution Symposium, Albi, France (1998).

[3] Herbert Weit, "Betriebsverhalten und Maßstabsvergrößerung von Ruhrwerkskugelmuhlen", Dissertation, Technical University of Braunschweig, (1987).

[4] W. Q. Yang, "Hardware Design of Electrical Capacitance Tomography Systems", *Meas. Sci. Technol.* **7**: 225-232 (1996).

[5] M. J. Rhodes, M. Sollaart, and X. S. Wang, "Flow Structure in a Fast Fluid Bed", *Powder Technol.* **99**: 194-200 (1998).

[6] T. Dyakowski, "Electrical Capacitance Tomography for Fluidized Bed Analysis", in **Frontiers in Industrial Process Tomography**, D. M. Scott and R. A. Williams, Eds. (AIChE, New York, 1995).

[7] F. T. Kühn, J. C. Schouten, R. F. Mudde, C. M. van den Bleek, and B. Scarlett, "Analysis of Chaos in Fluidization Using Capacitance Tomography", *Meas. Sci. Technol.* **7**: 361-368 (1996).

[8] R. Mann, R. A. Williams, T. Dyakowski, F. J. Dickin, and R. B. Edwards, "Development of Mixing Models Using Electrical Resistance Tomography", *Chem. Eng. Sci.* **52**: 2073-2085 (1997).

[9] S. L. McKee, T. Dyakowski, R. A. Williams, and T. A. Bell, "Tomographic Imaging of Pneumatic Conveying Processes", *Proceedings of 1993 ECAPT, Karlsruhe, Germany*, pp.89-92 (1993).

[10] E. A. Hammer and R. G. Green, "The Spatial Filtering Effect of Capacitance Transducer Electrodes", *J. Phys. E: Sci. Instrum.* **16**: 438-442 (1983).

[11] W. Q. Yang, M. S. Adam, R. Watson, and M. S. Beck, "Monitoring Water Hammer by Capacitance Tomography", *Electr. Lett.* **32**: 1778-1779 (1996).

[12] H. Conrad, Y. Li, and Y. Chen, "The Temperature Dependence of the Electrorheology and Related Electrical Properties of Corn Starch/Corn Oil Suspensions", *J. Rheol.* **39**: 1041-1057 (1995).

[13] A. Plaskowski, M. S. Beck, R. Thorn, and T. Dyakowski, **Imaging Industrial Flows** (Institute of Physics Publishing, Bristol, 1995).